I. Introduction

Studies of the supernova remnants (SNRs) in the Large Magellanic Cloud (LMC) are essential to elucidate details of SNR evolution, nucleosynthesis, and the nature and environments of supernova progenitors. As probes of the interstellar medium (ISM), SNRs yield information on the energy balance and chemical composition of their environments, which serves as input to larger questions of galactic chemical evolution and the star formation history of the Cloud. The relative closeness of the LMC plus its well-determined distance (50 kpc) means that accurate physical quantities can be derived for individual remnants in the galaxy. Also, due to the modest interstellar absorption toward the LMC, it is possible to detect X-rays in the important 0.5–2.5 keV energy band, which includes emission lines from the most abundant metals in the Universe, such as K-shell transitions of highly-ionized atoms of O, Ne, Mg, Si, and S and L-shell lines of ionized Fe.

The goals of our proposed new AXAF observations of the LMC SNRs are to (1) improve on *ASCA*–derived metal abundances in the gas phase of the LMC; (2) confirm the existence of newly processed metals in the interiors of middle-aged SNRs and study the amount and spatial distribution of these ejecta; (3) find and study power-law X-ray emission components that might arise from nonthermal distributions of electrons in pulsar-powered synchrotron nebula or originating through shock acceleration; (4) clarify the evolutionary state of the remnants to better understand the progenitor stars and their effects on the local environment.

Table 1 presents a size-ordered list of all thermal X-ray–emitting LMC SNRs brighter than $\sim 10^{-11}$ erg s^{-1} cm^{-2} over 0.15–4.0 keV. The 3 GTO targets are not being re-proposed here. Our group has access to two of them through our own GTO time (N103B) or through a long-standing collaboration with C. Canizares (N132D) and we will include these 2 important objects in our systematic study from the start. The remaining GTO target (0519−69.0) will be included when the AXAF data become publically available. The physical sizes in Table 1 correspond to angular sizes of $12''$ to $70''$, which makes them ideal targets for AXAF. Our ACIS-I count rates come from our detailed analysis of *ASCA* SIS data. We propose 40 ks observations of each target (50 ks for 0509−67.5, because of its low count rate and scientific importance) to obtain at least 2 times (for 0509−67.5, 3×; and N63A, 4×) more events than in our *ASCA* observations. We chose the ACIS-I to get the best spectral resolution and calibration and lowest background. Even integrated over the remnant, background in AXAF will still be a factor of 10 (for N49B) to 250 (for 0509−67.5) times less than for *ASCA*, allowing us to detect and study the important emission above ∼3 keV that was overwhelmed by background in *ASCA*. N49 and N49B are separated by merely $6\farcm7$, so they can be observed in a single pointing with no loss of imaging performance.

II. Summary of *ASCA* Results

Hughes et al. (1995, ApJ, 444, L81) first presented the *ASCA* X-ray spectra of 0509−67.5, 0519−69.0 and N103B, which showed strong Kα emission lines of Si, S, Ar, and Ca and no evidence for corresponding lines of O, Ne, or Mg. The dominant spectral feature was a broad blend of Fe L-shell emission lines (near 1 keV, see Fig. 1). The spectra were qualitatively consistent with model calculations of nucleosynthesis in Type Ia supernovae (SNe) (Nomoto et al. 1984, ApJ, 286, 644), but were inconsistent with nucleosynthetic yields from Type Ib and II SNe. From this evidence we concluded that the SNe which produced these remnants were of Type Ia, which confirmed earlier suggestions that the class of Balmer-dominated remnants arise from Type Ia SN explosions.

We recently completed a detailed analysis of the seven SNRs listed at the bottom of Table 1 (Hughes et al. 1998, in prep.). We fitted self-consistent nonequilibrium ionization (NEI) Sedov phase SNR models to the *ASCA* SIS data. The model was parameterized by the column density, shock temperature, ionization timescale, emission measure, and elemental abundances. All the remnants were adequately described by the model, allowing us to derive reasonable values for their physical parameters, i.e., ages, densities, initial explosion energies. A restricted subset of the sample (N23, N49, DEM71, and 0453−68.5), for which the ionization and Sedov dynamical ages agree quite well assuming the electron and ion temperatures are not fully equilibrated at the shock front (which seems to be the favored model currently), yield a mean value of the initial SN explosion energy of $(1.1 \pm 0.5) \times 10^{51}$ erg. We show that it is likely that the other three remnants (N63A, N132D,

Table 1 Thermal X-ray Emitting SNRs in the LMC							
Source	Common Name	Radius (pc)	kT (keV)	F_x (erg s^{-1} cm^{-2})	Observation Time (ks)	ACIS-I Events	Priority
0509−68.7	N103B	3.0	1.13	4.9×10^{-11}	(40)	...	GTO
0509−67.5	...	3.3	1.24	0.9	50	36000	1
0519−69.0	...	3.6	1.48	2.9	(55)	...	GTO
0506−68.0	N23	6.7	0.56	1.8	40	51600	5
0525−66.1	N49	8.2	0.60	5.3	40	90800	4
0535−66.0	N63A	8.5	0.65	15.1	40	460000	3
0505−67.9	DEM71	10.4	0.82	2.8	40	70800	2
0525−69.6	N132D	12.1	0.73	22.9	(100)	...	GTO
0453−68.5	...	15.0	0.61	0.9	40	20000	6
0525−66.0	N49B	17.0	0.43	2.4	40	48400	4

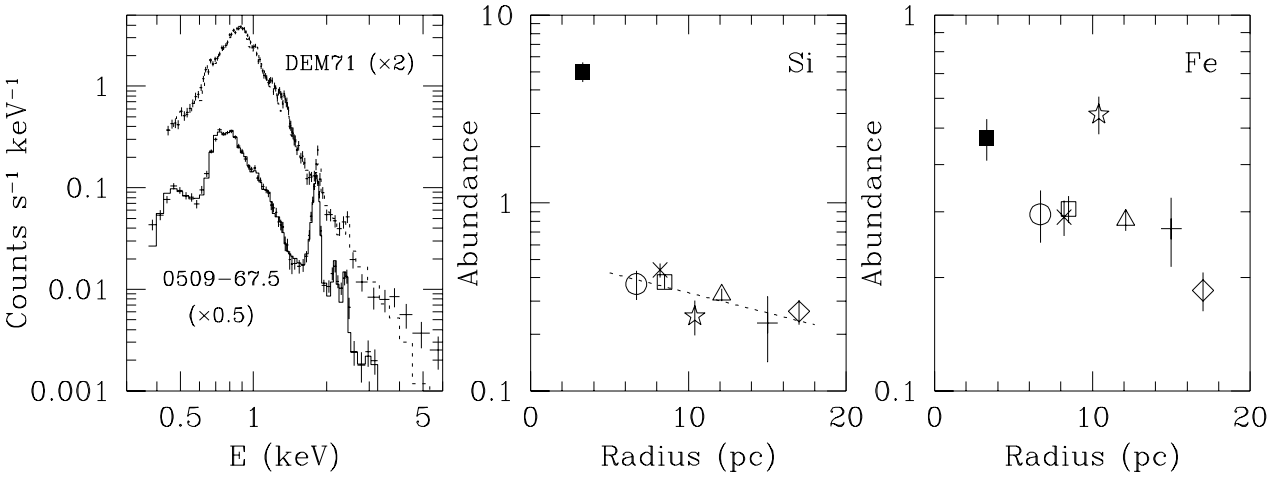

Figure 1 (Left) – *ASCA* X-ray spectra of 0509−67.5 and DEM71, the remnants of Type Ia SNe. The spectra have been scaled as indicated for clarity. Note the huge Si He-like Kα emission line ($E \sim 1.85$ keV) of 0509−67.5.
Figure 2 (Middle) – Silicon abundances derived from *ASCA* X-ray spectroscopy of LMC SNRs. Values for eight remnants are shown using different symbols: the filled square, circle, cross, open square, star, triangle, plus sign, and diamond correspond to 0509−67.5, N23, N49, N63A, DEM71, N132D, 0453−68.5, and N49B, respectively.
Figure 3 (Right) – Iron abundances derived from *ASCA* X-ray spectroscopy of LMC SNRs. Same symbols as for Figure 2. Note the anomalously high abundance for DEM71 (star symbol at $R \sim 10$ pc).

and N49B) exploded within preexisting cavities in the ISM (although by now the SN blast wave has lit up the cavity walls) because of their large inferred explosion energies ($>3 \times 10^{51}$ erg) and discrepancy between their ionization and Sedov dynamical ages. This has been suspected to be the case for N132D because of a discrepancy between the Sedov dynamical age and the kinematic age from the expanding high velocity oxygen-rich filaments (Hughes 1987, ApJ, 314, 103). Our independent estimate of N132D's age from its ionization timescale confirms this earlier result and it gives confidence that N63A and N49B are actually two more examples of this phenomenon.

We find statistical evidence for enrichment by supernova ejecta in the sense that smaller remnants show a somewhat higher mean metallicity than the larger ones. In the case of DEM71 (see spectrum in Fig. 1), which is Balmer-dominated and thus the remnant of a Type Ia supernova, the derived abundance of Fe is about a factor of two larger than the other remnants in the sample (see Fig. 3). All things being considered, however, the middle-aged, evolved SNRs are in general dominated by swept-up ISM and so can be used to estimate the mean LMC gas-phase abundances. We find that the common elements from O to Fe have abundances 0.2–0.4 times solar, consistent

with previous results based on optical and UV data, but without the anomalous overabundance of Mg and Si seen by Russell & Dopita (1992, ApJ, 384, 508).

These results are based on the analysis of globally averaged *ASCA* spectra. SNR X-ray spectra are complicated by NEI, lack of equilibration between electron and ion temperatures, emission from SN ejecta, complex morphologies, variations of the hot gas properties with position, and the presence of localized regions with power-law emission. We have accounted for the first two effects in the context of Sedov evolution and have identified the presence of SN ejecta in some of the remnants. However, because of the broad PSF of *ASCA* and the limited spectral resolution of *ROSAT*, exploration of the remaining issues has been impossible until now. ACIS-I provides the high spatial resolution and spectral resolution that makes it possible to study the spatial variations of the hot gas in SNRs and thereby test the assumptions made in our earlier work (e.g., Sedov evolution), improve our estimates of the LMC abundances, discover ejecta emission directly, and map regions of nonthermal X-ray emission. Below we outline in more detail two important scientific programs that we intend to accomplish with the proposed observations.

III. Nucleosynthesis, Ejecta, and the Abundances of the LMC

a. Remnants of Type Ia SNe: 0509−67.5 and DEM71

As the source of most of the Fe in the Universe, Type Ia SNe play a fundamental role in the chemical evolution of galaxies, which makes studies of remnants of Ia's throughout their evolution of great importance. SNRs 0509−67.5 and DEM71 are particularly valuable because they are among the youngest and oldest such Ia remnants in the LMC, which means they provide an unprecedented opportunity to study the time evolution of Type Ia SN ejecta. Figs. 2 and 3 show that 0509−67.5 (filled square symbol) is greatly enriched in Si but only slightly enriched in Fe, while the middle-aged ($t \sim 5000$ yr) SNR DEM71 (open star symbol) shows normal Si, but a factor of two enhanced Fe compared to other similar-sized SNRs. Immediately this indicates that Type Ia SN ejecta are stratified by composition (Fe inside Si) and for DEM71 we get a very coarse estimate of $\sim 0.1\,M_{\odot}$ for the mass of Fe. To improve on these results we must determine how the excess Fe in DEM71 is distributed (near the edge or center, in clumps or uniformly), and identify if other species (Si, Ar) are enhanced. For 0509−67.5, measurements of the Ar and Ca abundances will probe the extent of stratification. It will also be critical to determine the blast wave velocity in 0509−67.5, since optical results only constrain it to be >2000 km s^{-1} (Smith et al. 1991, ApJ, 375, 652). This will be challenging even for AXAF since it requires extracting and analyzing the X-ray spectrum of the outward moving shock in the ambient ISM, which is predicted to be faint and not well resolved from the ejecta component. We note that we have Hα optical images of these SNRs already and will propose to use the Rutgers Fabry-Perot to search for coronal [Fe XIV] λ5303 emission as well.

b. The Evolved LMC SNRs

Based on the *ASCA* results, the other evolved LMC SNRs do not show evidence individually for the presence of X-ray–emitting SN ejecta. Yet, when considered as a sample, there is a significant correlation between the remnant radii and mean metallicities, with the smaller SNRs (N23, N49, and N63A) showing higher abundances than the larger ones (0453−68.5 and N49B) (see the dotted line in Fig. 2). It is not entirely clear why the metallicities correlate so well with radius and not with the amount of swept-up mass, but this must be telling us about the complex fate of the metals ejected by a SN (see Tenorio-Tagle 1996, AJ, 111, 1641). AXAF imaging will allow us to make very sensitive searches for direct evidence of the ejecta component in these SNRs (using line ratio maps and direct spectral fits, as appropriate) and to determine its amount and distribution.

Once the spatial regions of these remnants that are polluted by SN ejecta are identified, we will utilize the remaining parts to determine the gas-phase abundances of the LMC. Eliminating this major source of systematic error (ejecta contamination) will result in more *accurate* abundance estimates than we derived earlier, while retaining comparable statistical *precision* (because our request is for *twice* the number of *ASCA* events). We will also search for evidence of the destruction of interstellar dust grains in the hot gas behind the supernova blast wave. Vancura et al. (1994, ApJ, 431, 18) predict that Mg, Si, Ca, and Fe should be entirely depleted from the gas phase at the shock front, and these species should appear in the X-ray spectra to a progressively greater extent

deeper into the remnant. Our ACIS-I observations will be very sensitive to such variations.

The Sedov models from our *ASCA* study predict a measureable radial variation in temperature: the projected kT at the SNR's center should be some 20% to 35% higher than kT at the edge. Our *ASCA* fit results provide the best guide to the expected precision of our ACIS-I temperature measurements. We found an excellent correlation between the number of events C in the *ASCA* spectra and the fitted kT uncertainty: $\sigma_{kT}/kT = 0.17(C/10^4)^{-0.67}$, even when allowing the column density, ionization timescale, emission measure, and abundances to vary freely. Thus if our Sedov models are correct, a definitive measurement of the radial kT gradient will be possible for N63A and will require ∼50000 events from each of 10 radial regions, which justifies our requested 40 ks observation. Since N63A is one of the SNRs that we propose exploded in a wind-blown cavity, comparing its observed radial variation of temperature against the Sedov model is a critical test. For the other remnants we will be sensitive to temperature variations of $\lesssim$50% over $\gtrsim$10 independent spatial regions.

IV. Pulsar-Powered Synchrotron Nebulae in LMC SNRs

X-ray imaging at energies above ∼4 keV has been arguably the most important recent development in the search for pulsar-powered synchrotron nebula (PSN) in supernova remnants. Studies with *ASCA* in the past 2 years have resulted in the discovery of PSN in, for example, W44 (Harrus, Hughes, & Helfand 1996, ApJ, 464, L161), CTA-1 (Slane et al. 1997, ApJ, 485, 221), and MSH 11-62 (Harrus, Hughes, & Slane 1998, astro-ph/9801204). The reason for this is simple: above 4 keV thermal emission from shock-heated gas is negligible, while hard power-law emission from a PSN remains relatively strong. The discovery of a PSN in a supernova remnant is pivotal, since it conclusively establishes the remnant as the product of a massive star core collapse SNe. The only LMC SNRs that can, without question, be put in this class are 0540−69.3 ($L_X \sim 10^{37}$ erg s^{-1}) and N157B ($L_X \sim 3\times10^{36}$ erg s^{-1}). A factor of >2500 separates the luminosity of 0540−69.3 from that of the faintest known Galactic PSN which surrounds PSR B1853+01 in W44.

We do not claim unambiguous detection of nonthermal X-ray emission for the LMC SNRs, because the *ASCA* emission observed above ∼2 keV is comparable to the fluctuations in background. However, the upper limits we set are very interesting, and correspond to soft X-ray luminosities for the nonthermal emission that range from lows of 2×10^{35} erg s^{-1} for N23, 0453−68.5, and N49B to a high of 1.4×10^{36} erg s^{-1} for N63A. These values are in the range expected for PSN.

For a power-law spectral index of $\alpha_p = -2$, ACIS-I count rates (2–8 keV) are 0.016–0.11 s^{-1} for the X-ray luminosities quoted above. The sizes of Galactic PSN ($R \sim 2.5$ pc) suggest angular sizes for LMC PSN of ∼10″, over which region the background rate will be essentially negligible (0.0017 s^{-1} over 2–8 keV). So our 40 ks observations will allow a 10-σ detection of a PSN with $L_x = 3\times10^{34}$ erg s^{-1} which is ∼10 times less than our smallest upper limit value.

The most likely remnants to contain PSNs are the 3 that our work suggests have exploded in wind-blown cavities in the ISM: N63A, N132D, and N49B. Of these N63A is the best candidate because of its high upper limit from *ASCA*, which is why we make this our third highest priority object. N49B and N49 are assigned the next highest priority. PSN also emit highly-polarized flat-spectrum radiation in the radio band. Of the remnants we are proposing for, we know of only one, N49, that has been studied with the Australia Telescope Compact Array (ATCA) at arcsecond resolution (searching, unsuccessfully, for a radio counterpart to the 1979 Mar 5 γ-ray burst) and no polarization data was presented (Dickel et al. 1995, ApJ, 448, 623). (By the way, our ACIS-I observation of N49 will be able to definitely determine the thermal/nonthermal nature of the X-ray "hot spot" near the γ-ray burst position and thereby resolve this long-standing issue.) We will pursue ACTA observations of promising PSN candidates that arise from our AXAF study.

Type Ia SNe should not contain PSN, but it is possible that they may show nonthermal X-ray emission from shock acceleration as observed in SN1006 (Koyama et al. 1995, Nature, 378, 255). This emission tends to be steeper spectrum ($\alpha_p = -2.4$ to -3) and fainter (SN1006's soft L_x is $\sim4\times10^{34}$ erg s^{-1}) than that of PSN and therefore is much more difficult to detect in LMC SNRs. Nevertheless we will carry out a sensitive search for this using our maximum-likelihood two-dimensional image fitting techniques and will follow-up with deeper observations later if warranted.